



# Supercritical fluid impregnation – An eco-friendly technique for the functionalization of bioaerogel with phenolic compounds from passion fruit waste

Erick Jarles Santos de Araujo<sup>a,b</sup>, Eupidio Scopel<sup>c</sup>, Camila Alves Rezende<sup>c</sup>,  
José Claudio Klier Monteiro Filho<sup>d</sup>, Rodney Alexandre Ferreira Rodrigues<sup>d</sup>, Julian Martínez<sup>a,\*</sup>

<sup>a</sup> Laboratório de Alta Pressão em Engenharia de Alimentos (LAPEA), Faculdade de Engenharia de Alimentos (FEA), Universidade Estadual de Campinas (UNICAMP), 13083-862, Campinas, SP, Brazil

<sup>b</sup> Instituto Federal de Educação, Ciência e Tecnologia da Bahia, Campus Barreiras, 47808-006 Barreiras, BA, Brazil

<sup>c</sup> Universidade Estadual de Campinas (UNICAMP), Instituto de Química, 13083-970 Campinas, SP, Brazil

<sup>d</sup> Centro Pluridisciplinar de Pesquisas Químicas, Biológicas e Agrícolas (CPQBA), Universidade Estadual de Campinas (UNICAMP), P.O. Box 6171, 13083-970 Campinas, SP, Brazil

## ARTICLE INFO

### Keywords:

Waste recovery  
Piceatannol  
Incorporation of bioactive compounds  
Green engineering  
Supercritical technology

## ABSTRACT

Supercritical fluid impregnation (SFI), an eco-friendly technique, was applied to incorporate phenolic compounds from passion fruit bagasse into corn starch bioaerogel. This work investigated the effect of depressurization rate, contact time, and the number of cycles of SFI on the functionalization of the bioaerogel. SFI was conducted in static operation mode at 65 °C and 37.5 MPa, evaluating the effect of depressurization rate (slow and fast), process time (0.5–10 h), and number of cycles in terms of total reducing capacity (TRC), antioxidant capacity (Oxygen Radical Absorbance Capacity – ORAC and Ferric Reducing Antioxidant Power - FRAP), and piceatannol content of the impregnated bioaerogel. In single-cycle SFI the best results for TRC ( $0.65 \pm 0.01$  mg GAE/g aerogel), FRAP ( $1.61 \pm 0.02$  mg TE/g aerogel), and ORAC ( $3.42 \pm 0.01$  mg TE/g aerogel) were obtained with a fast depressurization rate and a contact time of 10 h. These results were surpassed when investigating the number of SFI cycles, with an increase of approximately 200 % in ORAC, 105 % in FRAP, and 330 % in the piceatannol content for SFI carried out with six 0.5 h cycles. The functionalization of corn starch bioaerogel with phenolic compounds from passion fruit waste by SFI offers a green engineering approach to obtain a high-value product with potential application in the pharmaceutical, nutraceutical, and food industries.

## 1. Introduction

Aerogels are multi-porous solid networks with low density, high surface area, extremely low thermal conductivity, high-temperature resistance, low refractive index, high transparency, and unique acoustic properties (Ganesan et al., 2018). Due to this set of characteristics, aerogels are materials with a wide range of applications. Aerogels are conventionally produced from synthetic or inorganic polymers; however, due to their negative environmental impact, aerogels made from biopolymers such as proteins and polysaccharides, known as bioaerogels, are gaining notoriety as sustainable alternatives (Budtova et al., 2020; Ganesan et al., 2018). In this scenario, starch, the second most abundant macromolecule in nature, is proving to be scientifically,

environmentally, and technically advantageous for producing bioaerogels. In addition, starch is cheap, bioavailable, non-toxic, and non-allergenic (Abdullah et al., 2022; García-González et al., 2015). The main sources of starch used in the production of bioaerogels are potatoes, peas, and corn. Corn starch has gained prominence due to its capability to form structured gels from the interaction between its molecules, amylose and amylopectin. Given their high porosity and surface area, corn starch bioaerogel have emerged as interesting matrices for the incorporation of bioactive compounds (Alavi & Ciftci, 2023; Baudron et al., 2020; Dias et al., 2022; Hatami et al., 2024; Mohammadi & Moghaddas, 2020; Zou & Budtova, 2021).

The extraction of bioactive compounds from agro-industrial wastes is a powerful strategy for developing highly economically viable processes

\* Corresponding author.

E-mail address: [julian@unicamp.br](mailto:julian@unicamp.br) (J. Martínez).

<https://doi.org/10.1016/j.foodres.2025.116637>

Received 23 December 2024; Received in revised form 22 April 2025; Accepted 11 May 2025

Available online 13 May 2025

0963-9969/© 2025 Elsevier Ltd. All rights are reserved, including those for text and data mining, AI training, and similar technologies.

and products (Nirmal et al., 2023). In addition, research into waste management is a relevant tool for promoting sustainable development and has been recognized as a promising approach towards a circular economy (Gavahian et al., 2021; Zhu et al., 2024). In this scenario, the extract obtained from yellow passion fruit (*Passiflora edulis* sp.) bagasse (PFB) has been reported as a source of bioactive compounds with high antioxidant capacity. Consisting of seeds and residual pulp, PFB is a little-explored source of phenolic compounds, especially piceatannol, a polyphenolic stilbene phytochemical and structural analogue of resveratrol (Matsui et al., 2010; Viganó et al., 2016; Viganó, de Assis, et al., 2020). Several works have attributed beneficial effects to piceatannol, including protection against skin and prostate cancer, preventing degenerative diseases, aiding vasodilation and metabolic health, and increasing the oxidative stability of food products (Baseggio et al., 2022; Bottoli & Da Silva, 2020; de Souza et al., 2022; Kinoshita et al., 2013; Kitada et al., 2017; Maruki-Uchida et al., 2013; Matsui et al., 2010; Santos et al., 2021).

Supercritical fluid impregnation (SFI), was recently applied for the incorporation of bioactive compounds from PFB extract into bioaerogel to protect them from deleterious factors, facilitate storage and transportation, and enable their application in controlled release systems (Araujo et al., 2023). SFI involves the mutual and complex interaction between a polymer matrix, a supercritical fluid, and the target compounds. In SFI, supercritical CO<sub>2</sub> (sc-CO<sub>2</sub>), the most commonly used supercritical fluid, solubilizes the target compounds and simultaneously promotes the swelling of the polymer matrix. Mass transfer is thus enhanced by the wider diffusive paths formed by swelling, and the target compounds are incorporated into the matrix by precipitation and adsorption. In addition, CO<sub>2</sub> is economically viable, non-flammable, non-toxic (considering typical outdoor concentrations, approximately 380 ppm), and can be easily removed by depressurization (Brunner, 2005; Clifford & Williams, 2000; De Corso et al., 2024; Gurikov & Smirnova, 2018; L. Ma et al., 2024; Weidner, 2018). Therefore, by replacing conventional solvents with CO<sub>2</sub> and minimizing adverse environmental effects, supercritical technologies such as SFI are presented as green technologies or eco-friendly alternatives (Alavi & Ciftci, 2024; Mottola et al., 2023a; Nalawade et al., 2006; Sheikh et al., 2025; Verano-Naranjo et al., 2025).

One of the main challenges of SFI is establishing the adequate operation conditions to preserve the bioactivity of the target compounds in the impregnated matrix. These conditions are directly related to the thermodynamic and kinetic properties of the system throughout the process. Therefore, finding the most suitable SFI conditions requires investigating parameters such as pressure, temperature, depressurization rate, contact time, operation mode, and process cycles, as well as acquiring knowledge on the solubility of the target compounds in sc-CO<sub>2</sub> (Belizón et al., 2018; Jordão et al., 2022; Sanchez-Sanchez et al., 2017).

Pressure and temperature are the most studied parameters in SFI, since they are related to the physicochemical, thermodynamic, and mass transfer properties of CO<sub>2</sub> (Fernandes et al., 2012; Friedman & Anderson, 2017; Santos et al., 2020; Villegas et al., 2020). In previous studies, we investigated the impact of pressure and temperature on the SFI technique for phenolic compounds from passion fruit bagasse extract (PFBE) incorporated into corn starch bioaerogel (Araujo et al., 2023). Subsequently, to investigate the solubility of PFBE in supercritical CO<sub>2</sub> (sc-CO<sub>2</sub>), we analyzed the behavior of the mixture (sc-CO<sub>2</sub> + PFBE) and evaluated the effects of different operating modes of the SFI technique (Araujo et al., 2024). However, based on the knowledge obtained in these studies, we identified the need for further research into parameters that have been little covered in the SFI technique, such as the depressurization rate and contact time.

The depressurization rate is based on the solubility of the components of interest in sc-CO<sub>2</sub>. Rapid depressurization is recommended for compounds with high solubility, which decreases solubility and helps precipitate the compound in the carrier material. For bioactive compounds with low solubility, slow depressurization is recommended if the

compound is solubilized in the supercritical phase for most of the process and the affinity with the polymer matrices greater than with the sc-CO<sub>2</sub> (Torres et al., 2014; Yokozaki et al., 2015). In addition, the depressurization rate is key in highlighting precipitation, a phenomenon not covered in most studies. Gurikov and Smirnova (2018) highlighted the importance of considering this phenomenon in SFI, stating that precipitation enables the rapid release of the impregnated target compounds, being an essential mechanism for specific applications that require this characteristic to fulfill their purposes.

Contact time is a parameter that demonstrates that SFI, as well as being influenced by thermodynamics, is also a kinetic process. In SFI, the time depends on the solubilization of the target compounds in sc-CO<sub>2</sub>, the diffusion of the supercritical solution (sc-CO<sub>2</sub> + target compounds) in the polymer matrix and possible structural reactions caused by the sorption of the sc-CO<sub>2</sub> in the polymer matrix. Generally, in order to maximize impregnation load, long contact times are used in SFI: 24 h (Kuska et al., 2019), 48 h (Franco et al., 2018) and 72 h (Drago et al., 2021). However, prolonged contact times present challenges for the application of SFI on an industrial scale. In addition, reducing energy consumption has been identified as a key strategy for environmental sustainability in industries (Zare Banadkouki, 2023). Therefore, one solution to this limitation is to carry out SFI in short cycles, an approach recently introduced in the literature (Dias et al., 2022). However, there are no records of its strategy in the SFI of natural extracts.

Seeking to offer a new perspective, this work aims to analyze the effect of depressurization rate, contact time, and SFI cycles to optimize the impregnation of PFBE in corn starch bioaerogels. In addition, the research was conducted based on a green engineering approach by integrating an emerging green technology (SFI), an agro-industrial waste (PFB), and a biopolymer (corn starch). Corn starch bioaerogels functionalized with phenolic compounds from PFBE by SFI are presented as potential candidates for exploitation by the food, nutraceutical, and pharmaceutical industries.

## 2. Materials and methods

### 2.1. Materials and reagents

2,4,6-Tris(2-pyridyl)-s-triazine (TPTZ, 98 %, Sigma-Aldrich, USA), 6-hydroxy-2,5,7,8-tramethylchro-mono-2-carboxylic acid (Trolox, 97 %, Sigma-Aldrich, USA), absolute ethanol (99.5 %, Dinâmica, São Paulo, Brazil), acetonitrile (99.9 %, J.T. Baker, Phillipsburg, NJ, USA), methanol (99.99 %, J.T. Baker, Phillipsburg, NJ, USA) carbon dioxide (99.99 %, White Martins, São Paulo, Brazil), Folin-Ciocalteu (Metaquímica, São Paulo, Brazil), fluorescein, 2-2'-azobis (2-methylpropion midene) dihydrochloride (APPH, 97 %, Sigma-Aldrich, USA), gallic acid, (97.5 %, Sigma-Aldrich, USA), piceatannol (98 %, Sigma-Aldrich, USA), trifluoroacetic acid (99.5 %, Sigma-Aldrich, USA) Span® 80 (surfactante, 0.99 g/mL at 20 °C, Sigma-Aldrich, USA). All chemicals were used as received. Ingredient Industry Ltda (São Paulo, Brazil) kindly donated corn starch (characterization available in the supplementary material, Fig. S34), and soybean oil (Liza, Cargill, Brazil) was purchased from a local supermarket (Campinas, São Paulo, Brazil).

### 2.2. Bioaerogel synthesis

The corn starch bioaerogel was synthesized in three stages, following the methodology proposed by De Marco et al. (2018), with some adaptations. The process was carried out in triplicate.

Stage 1: Initially, two solutions (A and B) were prepared. Solution A consisted of an aqueous suspension of corn starch at a concentration of 15 % by weight/volume (w/v), whereas Solution B was a mixture of soybean oil and Span® 80, used as an emulsifier, at a concentration of 2 % by weight/weight (w/w). Afterwards, Solution B was gradually added to Solution A, under constant stirring at 600 rpm and a temperature of 110 °C, in a volumetric ratio of 1:3 (Solution A: Solution B) to start the

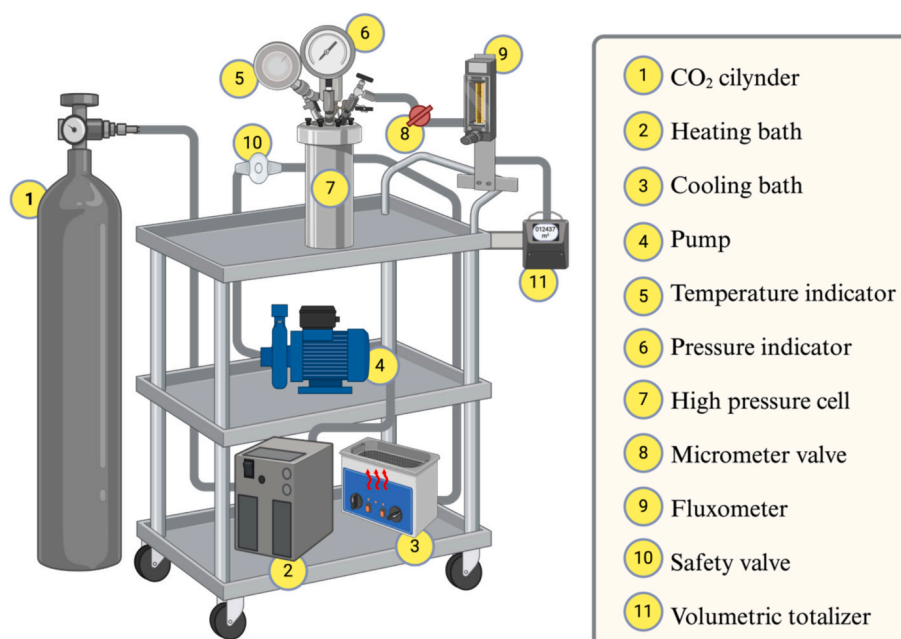


Fig. 1. Basic layout of the SFI unit.

gelatinization process. Stirring was maintained at 600 rpm and 110 °C for 2 h, ensuring complete gelatinization of the mixture and formation of the hydrogel. After gelatinization, the mixture was left to stand at room temperature for 1.5 h. The hydrogel was then stored at 4 °C for 72 h, allowing retrogradation, an essential process for stabilizing the hydrogel structure. After the retrogradation period, ethanol and water (30 % v/v) were added to the hydrogel to remove the oily phase. The oily phase was separated by decantation. Finally, the excess residual water was removed by subjecting the decanted material to vacuum filtration.

**Stage 2: Solvent exchange.** The solvent exchange was carried out by immersing the hydrogel particles in ethanol/water mixtures with increasing ethanol concentration (30 %, 60 %, 90 %, and 100 % v/v). The particles were weighed, and the solvent volume was equivalent to five times the initial mass. The solvent was changed every 24 h, and the last change (100 % v/v) was repeated thrice. In the third repetition using ethanol (100 % v/v), the particles remained in the solvent until being subjected to supercritical drying.

**Stage 3: Supercritical drying.** Supercritical drying was carried out according to Hatami et al. (2020), with some modifications. Initially, the excess of ethanol was removed from the container (glass laboratory flask graduated with screw cap, 250 mL capacity) of Stage 2 (solvent exchange) using a pipette, and the alcohol gel particles were added to a stainless-steel high-pressure cell (HPC) to remove the ethanol and obtain the aerogel. Supercritical drying was carried out at  $40 \pm 1$  °C and  $12 \pm 0.5$  MPa; these conditions were maintained until the solvent/particle mass ratio (S/F) reached 25 kg solvent/kg particle.

### 2.3. Production of the passion fruit bagasse extract

PFBE was produced as described by Viganó et al. (2016). The dried and crushed PFB was first defatted by supercritical fluid extraction (SFE) with CO<sub>2</sub> at  $35 \pm 1$  MPa and  $40 \pm 2$  °C. Then, the defatted PFB underwent pressurized liquid extraction (PLE) using ethanol (99 %) at  $10 \pm 1$  MPa and  $75 \pm 2$  °C.

### 2.4. Supercritical fluid impregnation (SFI)

Fig. 1 shows the basic layout of the SFI unit used in this work. Initially, 150 mg of the corn starch bioaerogel was added to an 18.70 mL glass beaker (internal diameter 2.3 cm) and inserted into a 100 mL HPC.

Table 1

Effect of depressurization rate and contact time on the SFI of phenolic compounds of PFBE in corn starch bioaerogel.

Condition	Contact time (h)	Depressurization rate (MPa/min)
1	0.5	1.03
2	0.5	7.54
3	1.0	1.03
4	1.0	7.54
5	2.0	1.03
6	2.0	7.54
7	3.0	1.03
8	3.0	7.54
9	5.0	1.03
10	5.0	7.54
11	10	1.03
12	10	7.54

Then, 3 mL of PFBE was carefully pipetted onto the HPC inner walls, avoiding prior contact with the bioaerogel. The HPC was closed, and the system was heated to 65 °C and pressurized to 37.5 MPa. SFI was carried out in static operation mode in a typical experiment for one process cycle. These conditions were optimized in a previous work (Araujo et al., 2023).

### 2.5. Effect of SFI parameters

The effect of the system's depressurization rate, contact time, and number of cycles on the SFI of PFBE in corn starch bioaerogel was evaluated. All experiments were carried out in duplicate.

#### 2.5.1. Effect of depressurization rate and contact time

The effect of the depressurization rate and contact time of the SFI of the phenolic compounds of PFBE on corn starch bioaerogel was evaluated based on the results of total reducing capacity (TRC), FRAP (ferric reducing antioxidant power) antioxidant capacity, and ORAC (oxygen radical absorbance capacity) antioxidant capacity. Twelve SFI conditions were investigated using seven contact times and two depressurization rates, as described in Table 1. The depressurization rates of 1.03 MPa/min and 7.54 MPa/min are named "slow" and "fast" in this work,

respectively. The technical and safety limitations of the SFI unit were considered for establishing the depressurization rates.

After SFI, the phenolic compounds impregnated in the bioaerogel were extracted using the method described by Buratto et al. (2019) with some modifications. First, the impregnated bioaerogel was immersed in ethanol (96 % purity) in a ratio of 0.05:1 (w/v). Next, the mixture (impregnated bioaerogel + ethanol) was subjected to magnetic homogenization for 15 min, followed by ultrasonic homogenization for 15 min. Finally, the bioaerogel particles were removed by filtration using a Chormafil Xtra PA-20/25 filter (Macherey-Nagel, Düren, Germany). The extract obtained was stored at  $-18^{\circ}\text{C}$ , protected from light, for future analysis.

**2.5.1.1. Total reducing capacity (TRC).** The TRC of the impregnated bioaerogel was assessed using the method of Singleton et al. (1999), with adaptations for microplate reading. Each microplate well was filled with 20  $\mu\text{L}$  of standard (0.02 to 0.20 mg/mL gallic acid), sample or blank. Then, 20  $\mu\text{L}$  of Folin-Ciocalteu reagent was added. After 3 min, 20  $\mu\text{L}$  of a saturated sodium carbonate solution and 140  $\mu\text{L}$  of distilled water were added. The microplate was incubated at room temperature and dark for 2 h. Finally, the absorbance was read at 760 nm using a FLUOstar Omega microplate reader (Bmg Labtech GmbH, Ortenberg, Germany). The results were processed using Omega Mars 3.32R5 data analysis software and expressed as mg of gallic acid equivalent (GAE) per g of sample.

**2.5.1.2. FRAP antioxidant capacity.** The FRAP (ferric reducing antioxidant power) of the impregnated bioaerogel was determined according to the method proposed by Benzie and Strain (1996) with adaptations. The FRAP solution was prepared by combining 20 mL of acetate buffer (0.3 M), 2 mL of TPTZ solution (10 mM), and 2 mL of ferric chloride solution (20 nM). The FRAP solution was protected from light and preheated to  $37^{\circ}\text{C}$ . Each well of the microplate was filled with 25  $\mu\text{L}$  of the sample, blank or standard (0.01–0.06 mg/mL Trolox solution) and 175  $\mu\text{L}$  of FRAP solution and pre-incubated in the dark at  $37^{\circ}\text{C}$ . After 0.5 h, the absorbance was read at 595 nm using a FLUOstar Omega microplate reader (BMG LABTECH GmbH, Ortenberg, Germany) with Omega Mars 3.32R5 data analysis software. The results were expressed in mg Trolox equivalent (TE) per g of sample.

**2.5.1.3. ORAC antioxidant capacity.** The ORAC (oxygen radical antioxidant capacity) method was applied according to the protocol described by Ou et al. (2013), with some modifications, to determine the antioxidant capacity of impregnated bioaerogel. 25  $\mu\text{L}$  of the sample, blank (75 mM phosphate buffer, pH 7.4) or standard (0.01–0.06  $\mu\text{g/mL}$  Trolox solution) were added to 150  $\mu\text{L}$  of fluorescein solution in each well of the black microplate. The microplate was incubated in the dark at  $37^{\circ}\text{C}$  for 15 min, after which 25  $\mu\text{L}$  of AAPH solution was added. The reduction in fluorescence (excitation at 485 nm; emission at 510 nm) was assessed in a FLUOstar Omega microplate reader (BMG LABTECH GmbH, Ortenberg, Germany) for 100 min at  $37^{\circ}\text{C}$ . Fluorescein solution served as a positive control, and the results were analyzed using Omega Mars 3.32R5 software and expressed in mg Trolox equivalent (TE) per mg of sample.

## 2.5.2. Effect of the number of SFI cycles

To investigate the effect of the number of cycles, the depressurization rate that obtained the best results in terms of TRC, ORAC, and FRAP (Section 2.5.1) and the shortest contact time were selected from those displayed in Table 1. Therefore, cycle 1 of SFI was carried out at  $65^{\circ}\text{C}$ , 37.5 MPa, 0.5 h of contact time, and fast depressurization rate. In cycle 2, after depressurizing the system from cycle 1, 3 mL of PBFE was added to the HPC, and SFI was carried out under the same conditions described for cycle 1. This procedure was carried out consecutively for seven cycles. Each cycle was evaluated in terms of the antioxidant capacity

(ORAC and FRAP) and piceatannol content of the impregnated bioaerogel. These results were also used to select the maximum number of cycles, considering the absence of significant differences or the decline in TRC, FRAP and ORAC between one cycle and the next.

**2.5.2.1. Quantification of piceatannol.** Piceatannol was quantified using the methodology proposed by Lai et al. (2013), with some adaptations, in a HPLC-DAD (High Performance Liquid Chromatograph - Diode Array Detector), Waters Alliance system (Waters Corp., Milford, MA, USA) with an automatic injector. A Waters Symmetry C18 column with an internal diameter of 100 mm  $\times$  2.1 mm and a particle size of 3.5  $\mu\text{m}$  (Milford, MA, USA) was used for the analysis of piceatannol. The mobile phases comprised water with 0.05 % trifluoroacetic acid (solvent A) and acetonitrile with 0.05 % trifluoroacetic acid (solvent B). The compounds were separated in the column at a temperature of  $40^{\circ}\text{C}$ , following the solvent gradient: 5 % B (0–35 min); 5–50 % B (35–40 min); 50–5 % B (40–55 min). The flow rate was 0.3 mL/min, and the injection volume was 10  $\mu\text{L}$ . The absorbance was recorded at 306 nm using a DAD. To carry out the injections, all the extracts were diluted in ethanol-HPLC grade, to a concentration of 1 mg/mL and filtered through a PVDF filter (Polyvinylidene Fluoride) Whatman® with a pore size of 0.45  $\mu\text{m}$ . The piceatannol calibration curve was obtained by a linear regression ( $y = 166,926x - 473,376$ ;  $R^2 = 0.9972$ ) using the same parameters as mentioned before, covering a concentration range of 1–200 ppm. The results were expressed in  $\mu\text{g}$  of piceatannol per g of bioaerogel, considering the volume/mass ratio between ethanol and impregnated bioaerogel used in the extraction process, using a ratio of 1 mL of ethanol per 50 mg of impregnated bioaerogel.

## 2.6. Physical characterization

The physical characterizations were carried out on the corn starch, the non-impregnated bioaerogel, and the impregnated bioaerogel samples selected from the evaluations of process time, depressurization rate, and cycles described in Sections 2.5.1 and 2.5.2.

### 2.6.1. Nitrogen adsorption/desorption

Approximately 100 mg of sample was used in the nitrogen adsorption/desorption measurements, with prior heating at  $60^{\circ}\text{C}$  under vacuum for 15 h. The measurements were carried out at 77 K (Quanta chrome Instruments, Nova 2200e). The Brunauer–Emmett–Teller (BET) method used a multi-point model to determine the surface area (relative pressure range from 0.05 to 0.3). The Barrett–Joyner–Halenda (BJH) method assessed the pore size distribution (relative pressure below 0.3).

### 2.6.2. Field emission scanning Electron microscopy (FESEM)

The morphology of the samples was analyzed using a high-resolution scanning electron microscope with an energy-dispersive X-ray detector (ThermoFisher Scientific UltraDry, ANAX-60P-B) operating at 4 kV. The samples were mounted on a metal platform and sprayed with gold coating under vacuum conditions, according to the methodology proposed by Li et al. (2021). More than ten images of each sample were taken to guarantee reproducibility.

## 2.7. Statistical analysis

The data was examined statistically using MINITAB® software (Version 16.1.0, Minitab Inc.). To identify significant differences at the 5 % level, analysis of variance (ANOVA) was performed using Tukey's test.



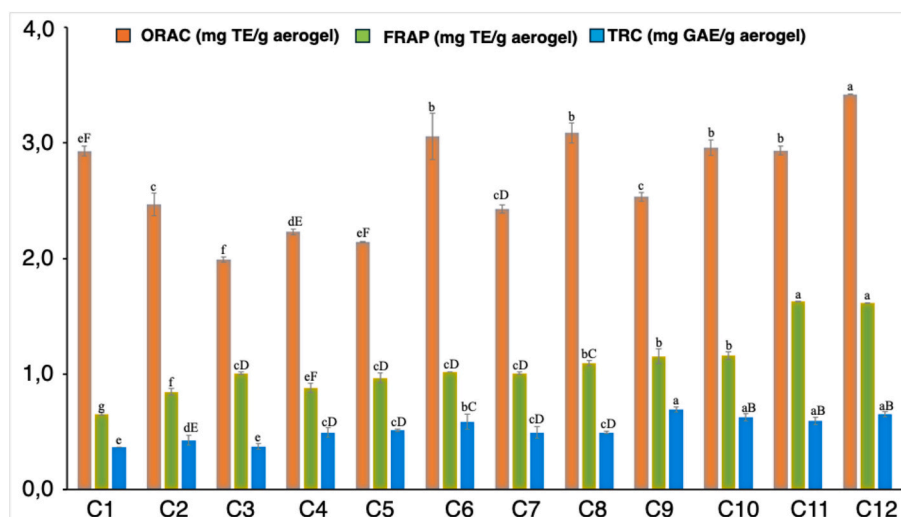


Fig. 2. Effect of the depressurization rate and contact time in the SFI of PFBE in corn starch bioaerogel. Conditions C1 to C12 are described in Table 1 (Section 2.5.1). Equal letters in columns with the same color indicate no statistical difference at the 95 % confidence level.

### 3. Results and discussion

#### 3.1. Effect of depressurization rate and contact time

Fig. 2 shows the results of the TRC, FRAP and ORAC antioxidant capacities obtained in the investigation of the effect of depressurization rate and contact time of SFI of PFBE on corn starch bioaerogel.

Regarding the effect of the depressurization rate, the ORAC antioxidant capacities achieved by fast depressurization were significantly higher than those obtained with the slow depressurization rate (1.03 MPa/min) for all the investigated SFI times. On the other hand, the TRC and FRAP results showed no significant differences at different depressurization rates. Fast depressurization rates are generally indicated for the SFI of target compounds with high solubility in sc-CO<sub>2</sub> since the rapid decrease in pressure promotes a reduction in solubility. This prevents the target compounds from being removed from the HPC along with the gaseous CO<sub>2</sub> and enhances their loading into the polymer matrix by precipitation (Gurikov & Smirnova, 2018; Singh et al., 2019; Yokozaki et al., 2015).

The observed behavior would not have been expected for the target compounds of this work since the phenolic compounds of PFB are polar and, therefore, have a low affinity for sc-CO<sub>2</sub> (de Melo et al., 2014). However, based on previous research (Araujo et al., 2023; Araujo et al., 2024), it was possible to find conditions related to the thermodynamic and operational SFI parameters (temperature, pressure, operating mode, and phase behavior) that overcame the solubility limitation imposed by the polarity of the PFBE phenolic compounds, making it possible to load them into bioaerogel by SFI. Thus, the results obtained for ORAC antioxidant capacity from SFI with a fast depressurization rate may be related to the incorporation of phenolic compounds into the bioaerogel by means of the precipitation phenomenon. This phenomenon occurs due to the phase change of CO<sub>2</sub> (from supercritical to liquid or vapor phase), triggered by an abrupt reduction in pressure in the system. This change results in a significant decrease in the solvating power of CO<sub>2</sub>, leading to the subsequent precipitation of the compounds of interest (Türk, 2014). Gurikov and Smirnova (2018) first highlighted the importance of considering precipitation phenomena in the SFI process; according to these authors, while slow depressurization favors impregnation from adsorption, rapid depressurization in porous polymeric materials can incorporate an additional amount of the target compound from precipitation, due to supersaturation and limitation in mass transfer within the pores. Recently, Hatami et al. (2024) also presented the importance of precipitation in the SFI of  $\beta$ -carotene.

In this scenario, the phenolic compounds precipitated in the bioaerogel are responsible for increasing the capacity to donate hydrogen atoms to free radicals, thus increasing the ORAC antioxidant capacity (Ou et al., 2013). The fact that this trend was not observed in the FRAP and TRC values suggests that the phenolic compounds in the PFBE, which can reduce both ferric ions from the FRAP method and *Folin-Ciocalteu* from the TRC method, have a different partition balance than those that were precipitated. In other words, these compounds have a greater affinity with the bioaerogel than with sc-CO<sub>2</sub> and were, therefore, not influenced by the rate at which CO<sub>2</sub> was removed from the system (Goñi et al., 2016; Torres et al., 2017). Therefore, these compounds were likely impregnated by adsorption. The antioxidant and reductive activity of the phenolic compounds present in PFBE result from their individual concentrations, chemical structures, and synergistic, antagonistic, or additive interactions (Skroza et al., 2022). The phenolic compounds in PFB were preliminarily identified by Santos et al. (2021). Although these authors used a higher temperature (110 °C) in PLE, the results may indicate the possible compounds in the PFBE used in this work. According to the results, PFB contains 25 phenolic compounds, mainly phenolic acids, flavonoids, stilbenes, carboxylic acids, and phenolic aldehydes. Among the most notable compounds are piceatannol, scirpusin B, resveratrol, citric acid, dihydroxybenzoic acid, caffeic acid, p-coumaric acid, catechin, acacetin, quercetin, flordizin and isomers of taxifolin I and II.

Recent works have also pointed out improved SFI conditions with a fast depressurization rate. Machado et al. (2024) achieved better conditions for the SFI of olive leaf phenolic extract in a polymer for medical applications using a fast depressurization rate (5 MPa/min). Similarly, Valor et al. (2023) demonstrated that the fast depressurization rate (5 MPa/min) was responsible for increasing the incorporation of mango leaf extract into conjugated polymer scaffolds via SFI.

In terms of contact time, when comparing the results obtained between 0.5 h (the shortest time evaluated) and 10 h (the longest time evaluated), using a fast depressurization rate, percentual increases of 51.16 % in TRC, 47.20 % in FRAP and 27.78 % in ORAC values were observed. Contact time is an important parameter in SFI because it influences the mass transfer from the supercritical solution (target compounds + sc-CO<sub>2</sub>) to the polymer matrix and depends on two stages. The first stage is the dissolution of the target compounds, and the second, the limiting stage, is related to their diffusion process (Guney & Akgerman, 2002). Understanding these steps in the SFI of multicomponent systems such as PFBE is complex, as it involves the dissolution of various phenolic compounds in sc-CO<sub>2</sub> and the achievement of their partition

**Table 2**

FRAP antioxidant capacity, ORAC antioxidant capacity, and piceatannol content ( $\mu\text{g/g}$  aerogel) of the bioaerogel obtained by SFI with different number of cycles.

Number of cycles	ORAC (mg TE/g aerogel)	FRAP (mg TE/g aerogel)	Piceatannol ( $\mu\text{g/g}$ bioaerogel)
1	$2.47 \pm 0.10^f$	$0.85 \pm 0.03^f$	$39.11 \pm 0.91^f$
2	$2.25 \pm 0.20^f$	$2.16 \pm 0.01^e$	$108.47 \pm 0.74^e$
3	$4.97 \pm 0.30^d$	$3.44 \pm 0.08^d$	$166.38 \pm 0.68^d$
4	$7.87 \pm 0.29^c$	$4.60 \pm 0.13^c$	$321.09 \pm 8.19^c$
5	$12.63 \pm 0.44^b$	$5.83 \pm 0.06^b$	$377.31 \pm 6.16^b$
6	$14.45 \pm 0.49^a$	$7.07 \pm 0.23^a$	$485.97 \pm 6.51^a$
7	$11.98 \pm 0.11^b$	$5.93 \pm 0.15^b$	$379.98 \pm 5.62^b$
SFI – C12	$3.42 \pm 0.20^e$	$1.61 \pm 0.01^g$	$113.33 \pm 2.22^e$

Different letters in the same column indicate a significant difference with 95 % confidence. C12: Condition in which SFI was carried out with a rapid depressurization rate and a contact time of 10 h.

equilibrium through the diffusive process. In addition, the mechanisms involved in the TRC, ORAC, and FRAP methods are closely related to the presence, concentration, and chemical structure of each phenolic compound and their mutual interactions, which can be synergistic, antagonistic, or additive (without interaction) (Skroza et al., 2022).

To evaluate the behavior of SFI at times longer than 10 h, an additional impregnation experiment was carried out at 37.5 MPa and 65 °C for 12 h with fast depressurization rate. The antioxidant capacities FRAP ( $1.13 \pm 0.03$  mg TE/g aerogel) and ORAC ( $2.37 \pm 0.28$  mg TE/g aerogel) were close to those obtained in SFI carried out for 5 h (also with fast depressurization) and lower than those obtained in 10 h. These results indicate that 10 h was enough time to achieve partition equilibrium between the phenolic compounds in the PFBE, sc-CO<sub>2</sub>, and the bioaerogel. Consequently, more extended periods favor the partition coefficient of the target compounds for sc-CO<sub>2</sub> rather than the bioaerogel, facilitating their removal with CO<sub>2</sub> during depressurization.

In SFI, contact time is also responsible for causing modifications in the polymer matrix, which may enhance diffusion as they make the polymer swell and plasticize. The time needed to achieve the swelling of the polymer matrix is related to its chemical structure. Some polymers require short periods of 2–3 h for swelling to be completed, whereas others need periods of up to 48 h (Belizón et al., 2018; Champeau, Thomassin, Tassaing, & Jérôme, 2015; Rojas et al., 2015; Sproule et al., 2004). SFI of the phenolic compounds of PFBE in starch bioaerogel achieved the best results with fast depressurization and contact time of 10 h, so this condition was chosen to investigate the effect of the number of SFI cycles and for the physical characterization of the bioaerogel.

### 3.2. Effect of the number of SFI cycles

Table 2 shows the FRAP antioxidant capacity, ORAC antioxidant capacity, and the piceatannol content of the impregnated bioaerogel produced by SFI at Condition C12 - the condition that obtained the best results in the investigation of depressurization rate and contact time (see Table 1) - and different numbers of cycles.

Increasing the number of cycles from 1 to 2 produced significant differences in the FRAP antioxidant capacity and the piceatannol content of the impregnated bioaerogel, representing a 155 % increase in FRAP and 177 % in the piceatannol content. A further increase from 2 to 3 cycles increased the ORAC antioxidant capacity by 121 %, the FRAP antioxidant capacity by 59 % and the amount of piceatannol by 53 %. The increase in ORAC, FRAP, and piceatannol content between cycles was maintained between cycles 3 and 4, 4 and 5, and 5 and 6. However, from cycle 6 to 7, there was a significant decrease in all the results, which is probably related to factors such as the reduction in the free active surface of the bioaerogel in the last cycle. The obstruction of the bioaerogel pores with the phenolic compounds incorporated in the previous six cycles hinders the diffusion of the supercritical solution

**Table 3**

Physical properties of corn starch and bioaerogel.

	Surface area (m <sup>2</sup> /g)	Average pore volume (cm <sup>3</sup> /g)	Average pore diameter (nm)
Corn starch	9.87	0.016	n.d.*
Non-impregnated bioaerogel	44.72	0.20	8.83
Impregnated bioaerogel (Fast depressurization, 10 h contact time)	36.55	0.15	8.35
Impregnated bioaerogel (6 cycles)	31.38	0.11	7.08

\* Not detected.

(phenolic compounds + sc-CO<sub>2</sub>) in the bioaerogel and the mass transfer during the seventh cycle. Due to the changes caused by six successive SFI cycles, the partial removal of the compounds incorporated in the previous cycles led to a partition coefficient more favorable to sc-CO<sub>2</sub> than to the bioaerogel, so these compounds were vented in the depressurization stage.

In addition, the results show that four SFI cycles of 0.5 h are sufficient to exceed the values obtained under condition C12, i.e., with 10 h of contact time. Moreover, the results obtained in cycle 6, compared to condition C12, correspond to an increase of approximately 200 % in ORAC antioxidant capacity, 105 % in FRAP antioxidant capacity, and 330 % in the piceatannol content. In addition to saving energy and time, the present study used a smaller aliquot of corn starch bioaerogel, 150 mg, and a lower total time related to the process cycles, three hours, than that performed by Dias et al. (2022), four hours, in the SFI of  $\beta$ -carotene.

The greatest amount of incorporated piceatannol in this work was 485.97  $\mu\text{g/g}$  of bioaerogel. A higher value, 741.85  $\mu\text{g/g}$  of aerogel, was obtained by Viganó, Meirelles, et al. (2020) when impregnating PFBE, but using the wet impregnation technique and a different polymer matrix, alginate aerogel. In addition to piceatannol, other phenolic compounds from PFBE were impregnated (Santos et al., 2021). These phenolic compounds are responsible for the bioactivity shown in the FRAP and ORAC antioxidant capacities, possibly increasing their concentrations as cycles increased from 1 to 6. Maintaining or increasing the bioactivity of the impregnated extract is considered a key factor in SFI. The physical-chemical interactions between the polymer matrix and the target compounds, such as hydrogen bonding, drive this factor (Champeau, Thomassin, Tassaing, & Jerome, 2015; Jordão et al., 2022; S.-L. Ma et al., 2010; Trindade Coutinho & Champeau, 2020).

### 3.3. Physical characterization of starch and bioaerogel

Surface area, volume, and average pore diameter values for corn starch, non-impregnated bioaerogel, bioaerogel impregnated with 10 h of contact time and fast depressurization rate (condition C12), and bioaerogel impregnated with six consecutive cycles are shown in Table 3.

The physical properties of the bioaerogel impregnated by SFI at the condition C12, compared to the non-impregnated bioaerogel, show a decrease of 8.17 m<sup>2</sup>/g in surface area, 0.04 cm<sup>3</sup>/g in average pore volume and 0.48 nm in average pore diameter. The bioaerogel impregnated with six SFI cycles showed more intense decreases, of 13.34 m<sup>2</sup>/g in surface area, 0.09 cm<sup>3</sup>/g in average pore volume, and 1.75 nm in average pore diameter. This trend suggests that the reductions in surface area, average pore volume, and average pore diameter are related to the incorporation of the phenolic compounds from PFBE into the corn starch bioaerogel. Buratto et al. (2019) also used nitrogen adsorption-desorption measurements to evaluate the impregnation of bioactive compounds from açai in silica aerogels and suggested that the decrease in the surface area of the impregnated aerogel was related to the filling of the pores of the aerogel with the açai extract. However, no decrease in

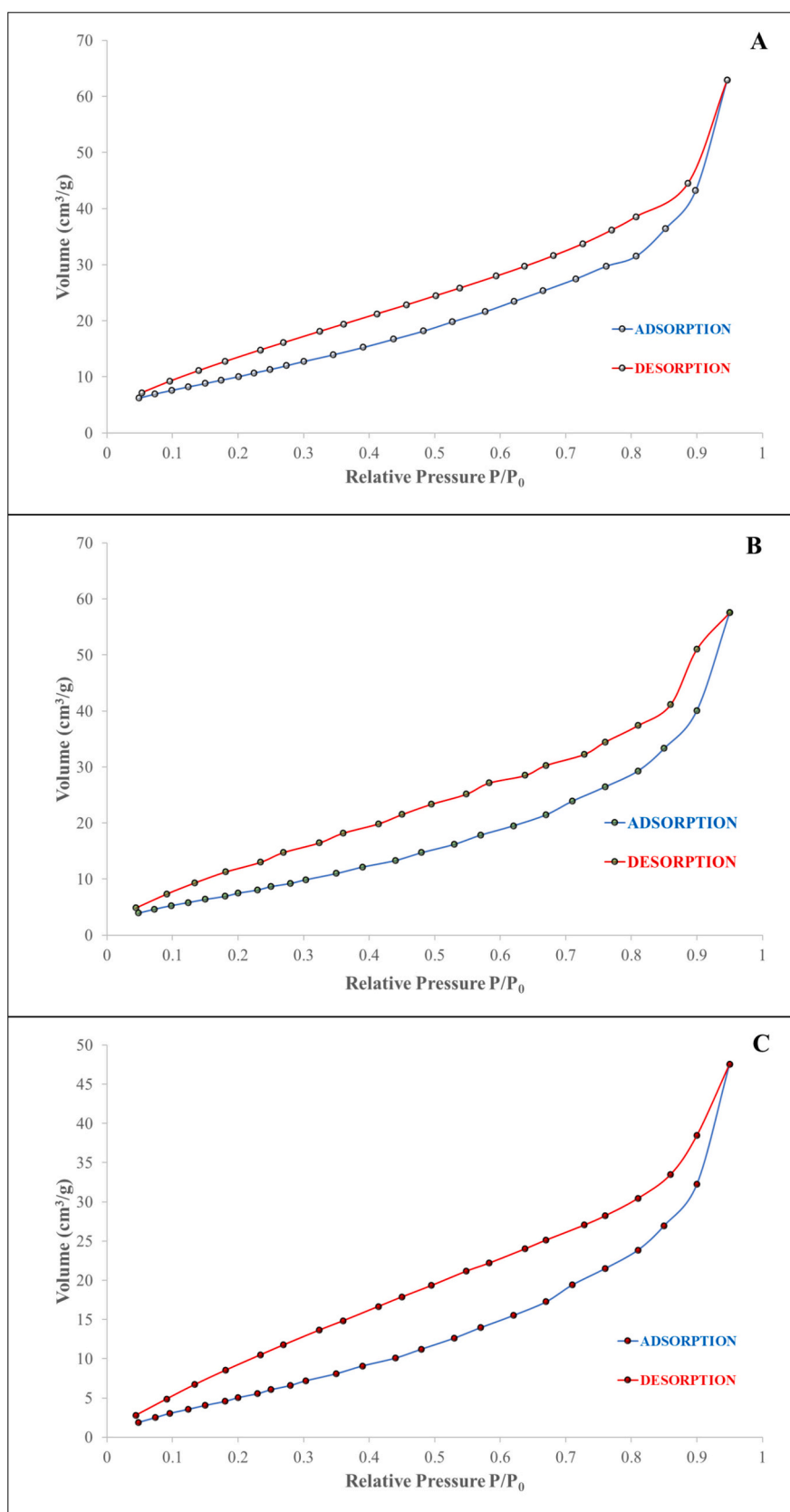


**Fig. 3.** Nitrogen adsorption-desorption isotherms for (A) non-impregnated bioaerogel; (B) bioaerogel impregnated by SFI with fast depressurization and 10 h of contact time; (C) bioaerogel impregnated with six SFI cycles.

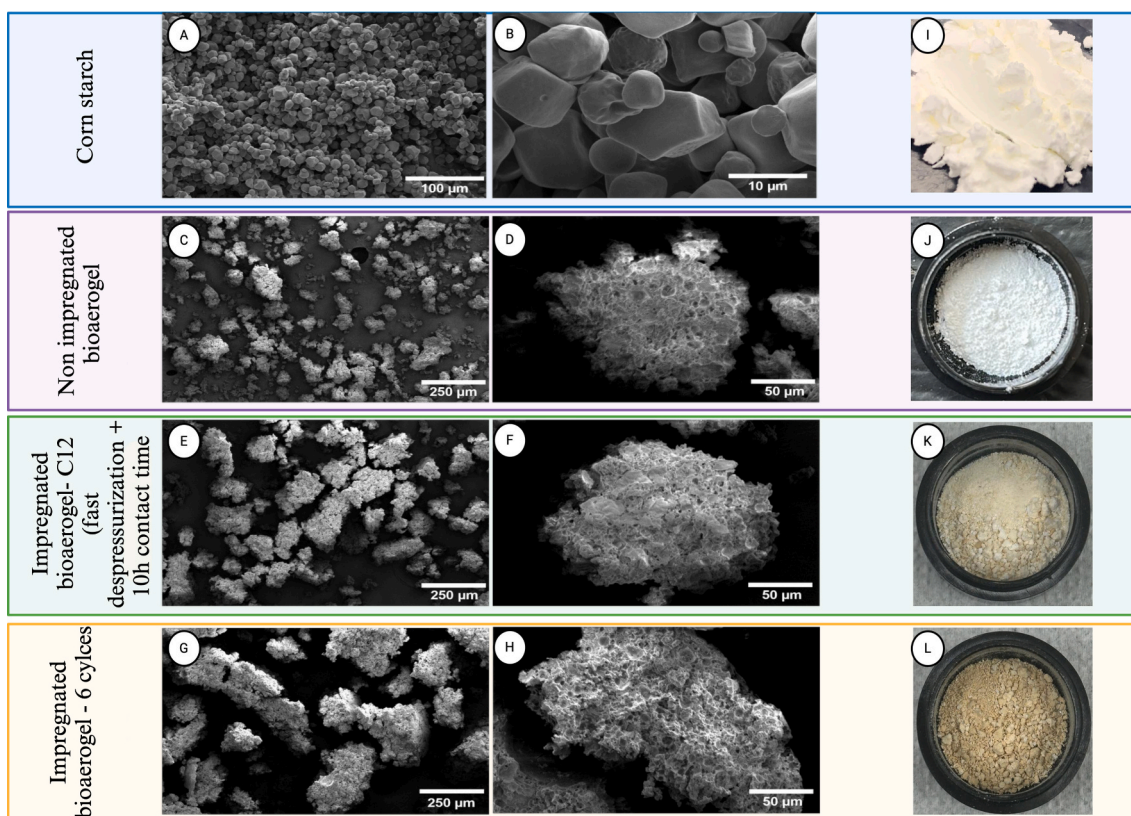


**Fig. 4.** Images obtained by FESEM and photographic images of corn starch (A, B and I); non-impregnated bioaerogel (C, D and J); bioaerogel impregnated by SFI with fast depressurization and 10 h of contact time (E, F and K); bioaerogel impregnated with six SFI cycles. (G, H and L).

the pore diameter was observed. In this scenario, it is important to note that the BJH approach carried out using the nitrogen adsorption-desorption method considers around 10 to 20 % of the total pore size of bioaerogel (Groult & Budtova, 2018; Rudaz et al., 2014).

The behavior of the adsorption and desorption isotherms obtained from the BJH approach is an indicative parameter of the pore characteristics in the materials. Fig. 3 shows the adsorption and desorption isotherms for the non-impregnated bioaerogel (Fig. 3A), the bioaerogel impregnated by SFI with fast depressurization and 10 h of contact time (Fig. 3B), and the bioaerogel impregnated with six SFI cycles (Fig. 3C). The adsorption isotherms of all the samples analyzed are classified by IUPAC as type II isotherms, with type H3 hysteresis loops typical of mesoporous adsorbent materials (Thommes et al., 2015). This same behavior was reported by Mottola et al. (2023a, 2023b) for potato and corn starch bioaerogel. The differences observed in the opening of the hysteresis loop suggest greater clogging of the pores of the bioaerogel impregnated with six cycles. In other words, the more significant obstruction of the bioaerogel pores, caused by the impregnation of compounds over the six cycles, resulted in a narrower opening in the hysteresis loop due to the difficulty imposed by obstructed pores in the adsorption and desorption process. This clogging indicates that, among the samples evaluated, the greatest amount of compounds impregnated in the bioaerogel was obtained with six consecutive SFI cycles. This aligns with the TRC and the antioxidant capacities (FRAP and ORAC) reported in Section 3.2.

Fig. 4 shows the respective FESEM images for corn starch, bioaerogel impregnated with fast depressurization and 10 h of contact time, and bioaerogel impregnated with six cycles. The raw corn starch is composed of non-porous particles (Fig. 4A, B), whereas the bioaerogel is composed of porous particles (Fig. 4C, D). Porosity is a possible effect of the gelification and drying processes used to prepare the bioaerogel. Interestingly, particles remain with the porous surface even after impregnation (Fig. 4E, F, G, H).

The images of the non-impregnated bioaerogel reveal an agglomeration of heterogeneous multi-porous particles. This phenomenon may be associated with the electrostatic interactions after the supercritical drying stage and the modifications caused by the emulsion gelation process (Alnaief et al., 2011). Despite the change in the visual appearance of the bioaerogel after SFI (Fig. 4J, K, L), it is not straightforward to detect the incorporation of phenolic compounds from PFBE into corn starch bioaerogel by FESEM, as most of the compounds may have been incorporated into regions that are difficult to observe using this technique or may have formed a very thin film onto particle surfaces. This same difficulty was reported by Belizón et al. (2018) in the SFI of antioxidant polyphenols from mango food-grade films. However, it is possible to observe an increase in particle agglomeration when comparing the images of the non-impregnated bioaerogel with those of the bioaerogel impregnated by SFI. This agglomeration may be related to the process of incorporating the phenolic compounds by SFI.

#### 4. Conclusion

The conditions for the functionalization of corn starch bioaerogel with the phenolic compounds of PFBE by SFI were improved by investigating the effects of depressurization rate, contact time and the number of process cycles. A fast depressurization rate achieved the best results in all the evaluated conditions. Regarding contact time, the greatest TRC ( $0.65 \pm 0.01$  mg GAE/g aerogel), FRAP antioxidant capacity ( $1.61 \pm 0.02$  mg TE/g aerogel), and ORAC antioxidant capacity ( $3.42 \pm 0.01$  mg TE/g aerogel) were obtained in 10 h. The analysis of the effect of the number of SFI cycles revealed that four cycles of 0.5 h are sufficient to exceed the TRC, FRAP, ORAC, and piceatannol content in the impregnated bioaerogel with fast depressurization and 10 h of contact time. Six SFI cycles achieved the greatest results of TRC, ORAC, FRAP and piceatannol content, as also indicated by nitrogen adsorption-desorption measurements. While the visual inspection of the samples indicated the



adsorption of PFBE and agreed with the chemical characterization of the impregnated bioaerogel, FESEM corroborated with the increase in porosity and did not reveal significant changes in their morphology after SFI. In conclusion, this work has shown the importance of investigating the effects of depressurization rate and contact time on the incorporation of phenolic compounds from PFBE into corn starch bioaerogel by SFI. In addition, the optimization of the number of SFI cycles is presented as a strategy to improve the process, since it can reduce the total operation time and increase the amount of incorporated target compounds. An eco-friendly technique (SFI), the recovery of an agro-industrial by-product (PFB), and the use of biopolymers were the pillars of this work for the production of a bioaerogel functionalized with bioactive compounds that can be applied in the pharmaceutical, nutraceutical, and food industries. Further studies into the applicability of bioaerogels and the controlled release of active compounds are essential to broaden knowledge on their potential and optimize their functionality.

### CRedit authorship contribution statement

**Erick Jarles Santos de Araujo:** Writing – original draft, Validation, Methodology, Investigation, Conceptualization. **Eupidio Scopel:** Methodology, Investigation. **Camila Alves Rezende:** Writing – original draft, Supervision, Funding acquisition. **José Claudio Klier Monteiro Filho:** Methodology, Investigation. **Rodney Alexandre Ferreira Rodrigues:** Writing – original draft, Supervision, Resources, Investigation, Funding acquisition. **Julian Martínez:** Writing – review & editing, Validation, Supervision, Resources, Project administration, Funding acquisition, Conceptualization.

### Declaration of competing interest

The authors declare that they have no known competing financial interests or personal relationships that could have appeared to influence the work reported in this paper.

### Acknowledgements

The authors would like to thank Conselho Nacional de Desenvolvimento Científico e Tecnológico (CNPq) [302968/2022-9], Fundação de Amparo à Pesquisa do Estado de São Paulo (FAPESP) [2019/19360-3, 2021/01008-1, 2023/17756-2] for financial support, the Instituto Federal de Educação, Ciência e Tecnologia da Bahia (IFBA) for granting a leave so that this work could be carried out, and Rafael Chelala Moreira for the help with the figures.

### Appendix A. Supplementary data

Supplementary data to this article can be found online at <https://doi.org/10.1016/j.foodres.2025.116637>.

### Data availability

Data will be made available on request.

### References

- Abdullah, Zou, Y. C., Farooq, S., Walayat, N., Zhang, H., Faieta, M., Pittia, P., & Huang, Q. (2022). Bio-aerogels: Fabrication, properties and food applications. *Critical Reviews in Food Science and Nutrition*, 0(0), 1–23. Doi: <https://doi.org/10.1080/10408398.2022.2037504>.
- Alavi, F., & Ciftci, O. N. (2023). Effect of starch type and chitosan supplementation on physicochemical properties, morphology, and oil structuring capacity of composite starch bioaerogels. *Food Hydrocolloids*, 141, Article 108637. <https://doi.org/10.1016/j.foodhyd.2023.108637>
- Alavi, F., & Ciftci, O. N. (2024). Increasing the bioavailability of curcumin using a green supercritical fluid technology-assisted approach based on simultaneous starch

- aerogel formation-curcumin impregnation. *Food Chemistry*, 455, Article 139468. <https://doi.org/10.1016/j.foodchem.2024.139468>
- Alnaief, M., Alzaitoun, M. A., García-González, C. A., & Smirnova, I. (2011). Preparation of biodegradable nanoporous microspherical aerogel based on alginate. *Carbohydrate Polymers*, 84(3), 1011–1018. <https://doi.org/10.1016/j.carbpol.2010.12.060>
- Araujo, E. J. S., Braga, A. J. O., Monteiro Filho, J. C. K., Ndiaye, P. M., Rodrigues, R. A. F., & Martínez, J. (2024). Supercritical fluid impregnation of phenolic compounds from passion fruit bagasse in corn starch aerogels: Phase behavior and effect of operation mode. *The Journal of Supercritical Fluids*, 214, Article 106387. <https://doi.org/10.1016/j.supflu.2024.106387>
- Araujo, E. J. S., Scopel, E., Rezende, C. A., & Martínez, J. (2023). Supercritical impregnation of polyphenols from passion fruit residue in corn starch aerogels: Effect of operational parameters. *Journal of Food Engineering*, 343, Article 111394. <https://doi.org/10.1016/j.jfoodeng.2022.111394>
- Baseggio, A. M., Kido, L. A., Viganó, J., Carneiro, M. J., de Lamas, C. A., Martínez, J., ... Maróstica Júnior, M. R. (2022). Systemic antioxidant and anti-inflammatory effects of yellow passion fruit bagasse extract during prostate cancer progression. *Journal of Food Biochemistry*, 46(3). <https://doi.org/10.1111/jfbc.13885>
- Baudron, V., Taboada, M., Gurikov, P., Smirnova, I., & Whitehouse, S. (2020). Production of starch aerogel in form of monoliths and microparticles. *Colloid and Polymer Science*, 298(4–5), 477–494. <https://doi.org/10.1007/s00396-020-04616-5>
- Belizón, M., Fernández-Ponce, M. T., Casas, L., Mantell, C., & Martínez De La Ossa-Fernández, E. J. (2018). Supercritical impregnation of antioxidant mango polyphenols into a multilayer PET/PP food-grade film. *Journal of CO2 Utilization*, 25, 56–67. <https://doi.org/10.1016/j.jcou.2018.03.005>
- Benzie, I. F. F., & Strain, J. J. (1996). The ferric reducing ability of plasma (FRAP) as a measure of “antioxidant power”: The FRAP assay. *Analytical Biochemistry*, 239(1), 70–76. <https://doi.org/10.1006/ABIO.1996.0292>
- Bottoli, C. B. G., & Da Silva, G. C. (2020). Process for obtaining passion fruit seed extract and its use in topical formulations (Patent BR 10 2020 013552 0 A2).
- Brunner, G. (2005). Supercritical fluids: Technology and application to food processing. *Journal of Food Engineering*, 67(1–2), 21–33. <https://doi.org/10.1016/J.JFOODENG.2004.05.060>
- Budtova, T., Aguilera, D. A., Beluns, S., Berglund, L., Chartier, C., Espinosa, E., ... Buwalda, S. J. (2020). Biorefinery approach for aerogels. *Polymers*, 12(12), 1–63. <https://doi.org/10.3390/polym12122779>
- Buratto, R. T., Hoyos, E. G., Cocero, M. J., & Martín, Á. (2019). Impregnation of açai residue extracts in silica-aerogel. *The Journal of Supercritical Fluids*, 146, 120–127. <https://doi.org/10.1016/j.supflu.2018.12.004>
- Champeau, M., Thomassin, J.-M., Tassaing, T., & Jérôme, C. (2015). Drug loading of polymer implants by supercritical CO<sub>2</sub> assisted impregnation: A review. *Journal of Controlled Release*, 209, 248–259. <https://doi.org/10.1016/j.jconrel.2015.05.002>
- Champeau, M., Thomassin, J.-M., Tassaing, T., & Jérôme, C. (2015). Drug loading of sutures by supercritical CO<sub>2</sub> impregnation: Effect of polymer/drug interactions and thermal transitions. *Macromolecular Materials and Engineering*, 300(6), 596–610. <https://doi.org/10.1002/mame.201400369>
- Clifford, A. A., & Williams, J. R. (2000). Introduction to supercritical fluids and their applications. In A. A. C. J. R. Williams (Ed.), *Supercritical fluid methods and protocols*. NJ: Humar.
- De Corso, A. R., De Carolis, A., Cornolti, L., Furlan, M., Widmer, P., Perale, G., ... Casalini, T. (2024). Drug loading of bioresorbable suture threads by supercritical CO<sub>2</sub> impregnation: A proof of concept for industrial scale-up. *The Journal of Supercritical Fluids*, 206, Article 106157. <https://doi.org/10.1016/j.supflu.2023.106157>
- De Marco, I., Iannone, R., Miranda, S., & Riemma, S. (2018). An environmental study on starch aerogel for drug delivery applications: Effect of plant scale-up. *International Journal of Life Cycle Assessment*, 23(6), 1228–1239. <https://doi.org/10.1007/s11367-017-1351-6>
- Dias, A. L. B., Hatami, T. V., Juliane, Santos de Araujo, E. J., Mei, L. H. I., Rezende, C. A., & Martínez, J. (2022). Role of supercritical CO<sub>2</sub> impregnation variables on  $\beta$ -carotene loading into corn starch aerogel particles. *Journal of CO2 Utilization*, 63 (June), Article 102125. <https://doi.org/10.1016/j.jcou.2022.102125>
- Drago, E., Campardelli, R., De Marco, I., & Perego, P. (2021). Optimization of PCL polymeric films as potential matrices for the loading of alpha-tocopherol by a combination of innovative green processes. *Processes*, 9(12). <https://doi.org/10.3390/pr9122244>
- Fernandes, J., Kjellow, A. W., & Henriksen, O. (2012). Modeling and optimization of the supercritical wood impregnation process—Focus on pressure and temperature. *The Journal of Supercritical Fluids*, 66, 307–314. <https://doi.org/10.1016/J.SUPFLU.2012.03.003>
- Franco, P., Aliakbarian, B., Perego, P., Reverchon, E., & De Marco, I. (2018). Supercritical adsorption of quercetin on aerogels for active packaging applications. *Industrial and Engineering Chemistry Research*, 57(44), 15105–15113. <https://doi.org/10.1021/acs.iecr.8b03666>
- Friedman, P., & Anderson, M. (2017). Thermodynamics. In *Fundamentals and applications of supercritical carbon dioxide (SCO2) based power cycles* (pp. 41–66). Elsevier. <https://doi.org/10.1016/B978-0-08-100804-1.00003-7>
- Ganesan, K., Budtova, T., Ratke, L., Gurikov, P., Baudron, V., Preibisch, I., ... Milow, B. (2018). Review on the production of polysaccharide aerogel particles. *Materials*, 11 (11), 2144. <https://doi.org/10.3390/ma11112144>
- García-González, C. A., Jin, M., Gerth, J., Alvarez-Lorenzo, C., & Smirnova, I. (2015). Polysaccharide-based aerogel microspheres for oral drug delivery. *Carbohydrate Polymers*, 117, 797–806. <https://doi.org/10.1016/j.carbpol.2014.10.045>
- Gavahian, M., Mathad, G. N., Pandiselvam, R., Lin, J., & Sun, D.-W. (2021). Emerging technologies to obtain pectin from food processing by-products: A strategy for

- enhancing resource efficiency. *Trends in Food Science & Technology*, 115, 42–54. <https://doi.org/10.1016/j.tifs.2021.06.018>
- Goñi, M. L., Gañán, N. A., Strumia, M. C., & Martini, R. E. (2016). Eugenol-loaded LLDPE films with antioxidant activity by supercritical carbon dioxide impregnation. *The Journal of Supercritical Fluids*, 111, 28–35. <https://doi.org/10.1016/J.SUPFLU.2016.01.012>
- Groult, S., & Budtova, T. (2018). Thermal conductivity/structure correlations in thermal super-insulating pectin aerogels. *Carbohydrate Polymers*, 196, 73–81. <https://doi.org/10.1016/j.carbpol.2018.05.026>
- Guney, O., & Akgerman, A. (2002). Synthesis of controlled-release products in supercritical medium. *AIChE Journal*, 48(4), 856–866. <https://doi.org/10.1002/aic.690480419>
- Gurikov, P., & Smirnova, I. (2018). Amorphization of drugs by adsorptive precipitation from supercritical solutions: A review. *The Journal of Supercritical Fluids*, 132, 105–125. <https://doi.org/10.1016/J.SUPFLU.2017.03.005>
- Hatami, T., Santos de Araujo, E. J., Luiz Baiao Dias, A., Helena Innocentini Mei, L., & Martínez, J. (2024). Mechanism of multicyclic  $\beta$ -carotene impregnation into corn starch aerogels via supercritical CO<sub>2</sub> with mathematical modeling. *Food Research International*, 178, Article 114002. <https://doi.org/10.1016/j.foodres.2024.114002>
- Hatami, T., Viganó, J., Innocentini Mei, L. H., & Martínez, J. (2020). Production of alginate-based aerogel particles using supercritical drying: Experiment, comprehensive mathematical model, and optimization. *The Journal of Supercritical Fluids*, 160, Article 104791. <https://doi.org/10.1016/J.SUPFLU.2020.104791>
- Jordão, A. M., Coutinho, I. T., Silva, E. K., Kato, I. T., Meireles, M. A. A., Silva, B. G., ... Champeau, M. (2022). Supercritical CO<sub>2</sub> impregnation of clove extract in polycarbonate: Effect of operational conditions on the loading and composition. *Processes*, 205, 10644. <https://doi.org/10.1016/j.supflu.2023.106144>
- Kinoshita, Y., Kawakami, S., Yanae, K., Sano, S., Uchida, H., Inagaki, H., & Ito, T. (2013). Effect of long-term piceatannol treatment on eNOS levels in cultured endothelial cells. *Biochemical and Biophysical Research Communications*, 430(3), 1164–1168. <https://doi.org/10.1016/j.bbrc.2012.12.017>
- Kitada, M., Ogura, Y., Maruki-Uchida, H., Sai, M., Suzuki, T., Kanasaki, K., ... Koya, D. (2017). The effect of Piceatannol from passion fruit (*Passiflora edulis*) seeds on metabolic health in humans. *Nutrients*, 9(10), 1142. <https://doi.org/10.3390/nu9101142>
- Kuska, R., Milovanovic, S., Frerich, S., & Ivanovic, J. (2019). Thermal analysis of polylactic acid under high CO<sub>2</sub> pressure applied in supercritical impregnation and foaming process design. *The Journal of Supercritical Fluids*, 144, 71–80. <https://doi.org/10.1016/J.SUPFLU.2018.10.008>
- Lai, T. N. H., Herent, M.-F., Quetin-Leclercq, J., Nguyen, T. B. T., Rogez, H., Larondelle, Y., & André, C. M. (2013). Piceatannol, a potent bioactive stilbene, as major phenolic component in *Rhodomyrtus tomentosa*. *Food Chemistry*, 138(2–3), 1421–1430. <https://doi.org/10.1016/j.foodchem.2012.10.125>
- Li, M., Wang, F., Wang, J., Wang, R., Strappe, P., Zheng, B., Zhou, Z., & Chen, L. (2021). Manipulation of the internal structure of starch by propionyl treatment and its diverse influence on digestion and in vitro fermentation characteristics. *Carbohydrate Polymers*, 270, Article 118390. <https://doi.org/10.1016/j.carbpol.2021.118390>
- Ma, L., Du, Y., Guo, X., Zhou, W., Deng, H., & Zhang, S. (2024). Process optimization of high purity CO<sub>2</sub> compression and purification system from oxygen-rich combustion flue gas. *International Journal of Greenhouse Gas Control*, 135, Article 104146. <https://doi.org/10.1016/j.ijggc.2024.104146>
- Ma, S.-L., Lu, Z.-W., Wu, Y.-T., & Zhang, Z.-B. (2010). Partitioning of drug model compounds between poly(lactic acid)s and supercritical CO<sub>2</sub> using quartz crystal microbalance as an in situ detector. *The Journal of Supercritical Fluids*, 54(2), 129–136. <https://doi.org/10.1016/j.supflu.2010.04.013>
- Machado, N. D., Mosquera, J. E., Cejudo-Bastante, C., Goñi, M. L., Martini, R. E., Gañán, N. A., ... Casas-Cardoso, L. (2024). Supercritical impregnation of PETG with *Olea europaea* leaf extract: Influence of operational parameters on expansion degree, antioxidant and mechanical properties. *Polymers*, 16(11), 1567. <https://doi.org/10.3390/polym16111567>
- Maruki-Uchida, H., Kurita, I., Sugiyama, K., Sai, M., Maeda, K., & Ito, T. (2013). The protective effects of piceatannol from passion fruit (*Passiflora edulis*) seeds in UVB-irradiated keratinocytes. *Biological and Pharmaceutical Bulletin*, 36(5), 845–849. <https://doi.org/10.1248/bpb.b12-00708>
- Matsui, Y., Sugiyama, K., Kamei, M., Takahashi, T., Suzuki, T., Katagata, Y., & Ito, T. (2010). Extract of passion fruit (*Passiflora edulis*) seed containing high amounts of piceatannol inhibits melanogenesis and promotes collagen synthesis. *Journal of Agricultural and Food Chemistry*, 58(20), 11112–11118. <https://doi.org/10.1021/jf102650d>
- de Melo, M. M. R., Silvestre, A. J. D., & Silva, C. M. (2014). Supercritical fluid extraction of vegetable matrices: Applications, trends and future perspectives of a convincing green technology. *The Journal of Supercritical Fluids*, 92, 115–176. <https://doi.org/10.1016/j.supflu.2014.04.007>
- Mohammadi, A., & Moghaddas, J. (2020). Mesoporous tablet-shaped potato starch aerogels for loading and release of the poorly water-soluble drug celecoxib. *Chinese Journal of Chemical Engineering*, 28(7), 1778–1787. <https://doi.org/10.1016/J.CJCHE.2020.03.040>
- Mottola, S., Iannone, G., Giordano, M., González-Garcinuño, Á., Jiménez, A., Tabernero, A., Martín del Valle, E., & De Marco, I. (2023). Supercritical impregnation of starch aerogels with quercetin: Fungistatic effect and release modelling with a compartmental model. *International Journal of Biological Macromolecules*, 253, Article 127406. <https://doi.org/10.1016/j.ijbiomac.2023.127406>
- Nalawade, S. P., Picchioni, F., & Janssen, L. P. B. M. (2006). Supercritical carbon dioxide as a green solvent for processing polymer melts: Processing aspects and applications. *Progress in Polymer Science*, 31(1), 19–43. <https://doi.org/10.1016/j.progpolymsci.2005.08.002>
- Nirmal, N., Khanashyam, A., Mundanat, A., Shah, K., Babu, K., Thorakkattu, P., ... Pandiselvam, R. (2023). Valorization of fruit waste for bioactive compounds and their applications in the food industry. *Foods*, 12(3), 556. <https://doi.org/10.3390/foods12030556>
- Ou, B., Chang, T., Huang, D., & Prior, R. L. (2013). Determination of total antioxidant capacity by oxygen radical absorbance capacity (ORAC) using fluorescein as the fluorescence probe: First action 2012.23. *Journal of AOAC International*, 96(6), 1372–1376. <https://doi.org/10.5740/jaoacint.13-175>
- Rojas, A., Cerro, D., Torres, A., Galotto, M. J., Guarda, A., & Romero, J. (2015). Supercritical impregnation and kinetic release of 2-nonanone in LLDPE films used for active food packaging. *The Journal of Supercritical Fluids*, 104, 76–84. <https://doi.org/10.1016/J.SUPFLU.2015.04.031>
- Rudaz, C., Courson, R., Bonnet, L., Calas-Etienne, S., Sallée, H., & Budtova, T. (2014). Aeropectin: Fully biomass-based mechanically strong and thermal superinsulating aerogel. *Biomacromolecules*, 15(6), 2188–2195. <https://doi.org/10.1021/bm500345u>
- Sanchez-Sanchez, J., Fernández-Ponce, M. T., Casas, L., Mantell, C., & de la Ossa, E. J. M. (2017). Impregnation of mango leaf extract into a polyester textile using supercritical carbon dioxide. *The Journal of Supercritical Fluids*, 128, 208–217. <https://doi.org/10.1016/j.supflu.2017.05.033>
- Santos, D. N., Aredo, V., Bazito, R. C., & de Oliveira, A. L. (2020). Water free incorporation of shark liver oil into starch microparticles by supercritical CO<sub>2</sub> impregnation at low temperature. *Journal of Food Process Engineering*, 43(11), 1–13. <https://doi.org/10.1111/jfpe.13541>
- Santos, L. C., Mendiola, J. A., del Sánchez-Camargo, A. P., Álvarez-Rivera, G., Viganó, J., Cifuentes, A., ... Martínez, J. (2021). Selective extraction of Piceatannol from *Passiflora edulis* by-products: Application of HSPs strategy and inhibition of neurodegenerative enzymes. *International Journal of Molecular Sciences*, 22(12), 6248. <https://doi.org/10.3390/ijms22126248>
- Sheikhi, A., Hamed, S., Sodeifian, G., & Razmimanesh, F. (2025). Improvement of the dissolution of the antineoplastic drug regorafenib through impregnation into pullulan polysaccharide using supercritical fluid technology: Optimization of the process. *Journal of CO<sub>2</sub> Utilization*, 93, Article 103040. <https://doi.org/10.1016/j.jcou.2025.103040>
- Singh, N., Mukhopadhyay, M., & Vinjamur, M. (2019). Analysis of modes of drug loading in silica aerogels from supercritical CO<sub>2</sub> solutions. *Journal of Supercritical Fluids*, 152, Article 104553. <https://doi.org/10.1016/j.supflu.2019.104553>
- Singleton, V. L., Orthofer, R., & Lamuela-Raventós, R. M. (1999). [14] Analysis of total phenols and other oxidation substrates and antioxidants by means of folin-ciocalteu reagent. *Methods in Enzymology*, 299, 152–178. [https://doi.org/10.1016/S0076-6879\(99\)99017-1](https://doi.org/10.1016/S0076-6879(99)99017-1)
- Skroza, D., Šimat, V., Vrdoljak, L., Jolić, N., Skelin, A., Čagalj, M., ... Generalić Mekinić, I. (2022). Investigation of antioxidant synergisms and antagonisms among phenolic acids in the model matrices using FRAP and ORAC methods. *Antioxidants*, 11(9), 1784. <https://doi.org/10.3390/antiox11091784>
- de Souza, M. P., de Amorim, F. D., Ferreira, M. R. A., Soares, L. A. L., & de Melo, M. A. (2022). Oxidative and storage stability in beef burgers from the use of bioactive compounds from the agro-industrial residues of passion fruit (*Passiflora edulis*). *Food Bioscience*, 48, Article 101823. <https://doi.org/10.1016/j.fbio.2022.101823>
- Sproule, T. L., Alex Lee, J., Li, H., Lannutti, J. J., & Tomasko, D. L. (2004). Bioactive polymer surfaces via supercritical fluids. *The Journal of Supercritical Fluids*, 28(2–3), 241–248. [https://doi.org/10.1016/S0896-8446\(03\)00044-5](https://doi.org/10.1016/S0896-8446(03)00044-5)
- Thommes, M., Kaneko, K., Neimark, A. V., Olivier, J. P., Rodríguez-Reinoso, F., Rouquerol, J., & Sing, K. S. W. (2015). Physisorption of gases, with special reference to the evaluation of surface area and pore size distribution (IUPAC Technical Report). *Pure and Applied Chemistry*, 87(9–10), 1051–1069. <https://doi.org/10.1515/pac-2014-1117>
- Torres, A., Ilabaca, E., Rojas, A., Rodríguez, F., Galotto, M. J., Guarda, A., ... Romero, J. (2017). Effect of processing conditions on the physical, chemical and transport properties of polylactic acid films containing thymol incorporated by supercritical impregnation. *European Polymer Journal*, 89, 195–210. <https://doi.org/10.1016/J.EURPOLYMJ.2017.01.019>
- Torres, A., Romero, J., Macan, A., Guarda, A., & Galotto, M. J. (2014). Near critical and supercritical impregnation and kinetic release of thymol in LLDPE films used for food packaging. *The Journal of Supercritical Fluids*, 85, 41–48. <https://doi.org/10.1016/J.SUPFLU.2013.10.011>
- Trindade Coutinho, I., & Champeau, M. (2020). Synergistic effects in the simultaneous supercritical CO<sub>2</sub> impregnation of two compounds into poly(L-lactic acid) and polyethylene. *The Journal of Supercritical Fluids*, 166, Article 105019. <https://doi.org/10.1016/J.SUPFLU.2020.105019>
- Türk, M. (2014). *Formation of organic particles using a supercritical fluid as solvent* (pp. 57–75). <https://doi.org/10.1016/B978-0-444-59486-0.00004-8>
- Valor, D., García-Casas, I., Montes, A., Danese, E., Pereyra, C., & de la Ossa, E. M. (2023). Supercritical impregnation of *Mangifera indica* leaves extracts into porous conductive PLGA-PEDOT scaffolds. *Polymers*, 16(1), 133. <https://doi.org/10.3390/polym16010133>
- Verano-Naranjo, L., Cejudo-Bastante, C., Casas, L., Lasanta, C., Freire, C. S. R., Vilela, C., & Mantell, C. (2025). Functionalization of a poly(lactic acid)/poly(butylene adipate-co-terephthalate)/thermoplastic starch film with olive leaf extract and its impact on postharvest green pepper quality. *Journal of Food Engineering*, Article 112582. <https://doi.org/10.1016/j.jfoodeng.2025.112582>
- Viganó, J., de Assis, B. F. P., Náthia-Neves, G., dos Santos, P., Meireles, M. A. A., Veggi, P. C., & Martínez, J. (2020). Extraction of bioactive compounds from defatted passion fruit bagasse (*Passiflora edulis* sp.) applying pressurized liquids assisted by

- ultrasound. *Ultrasonics Sonochemistry*, 64(December 2019), Article 104999. <https://doi.org/10.1016/j.ultsonch.2020.104999>
- Viganó, J., Meirelles, A. A. D., Náthia-Neves, G., Baseggio, A. M., Cunha, R. L., Maróstica Junior, M. R., ... Martínez, J. (2020). Impregnation of passion fruit bagasse extract in alginate aerogel microparticles. *International Journal of Biological Macromolecules*, 155, 1060–1068. <https://doi.org/10.1016/j.ijbiomac.2019.11.070>
- Viganó, J., Coutinho, J. P., Souza, D. S., Baroni, N. A. F., Godoy, H. T., Macedo, J. A., & Martínez, J. (2016). Exploring the selectivity of supercritical CO<sub>2</sub> to obtain nonpolar fractions of passion fruit bagasse extracts. *Journal of Supercritical Fluids*, 110, 1–10. <https://doi.org/10.1016/j.supflu.2015.12.001>
- Villegas, M. E., Aredo, V., Asevedo, K. J. E., Lourenço, R. V., Bazito, R. C., & Oliveira, A. L. (2020). Commercial starch behavior when impregnated with food additives by moderate temperature supercritical CO<sub>2</sub> processing. *Starch/Staerke*, 72(11–12), 1–11. Doi: <https://doi.org/10.1002/star.201900231>.
- Weidner, E. (2018). Impregnation via supercritical CO<sub>2</sub>—what we know and what we need to know. *Journal of Supercritical Fluids*, 134(December 2017), 220–227. <https://doi.org/10.1016/j.supflu.2017.12.024>
- Yokozaki, Y., Sakabe, J., Ng, B., & Shimoyama, Y. (2015). Effect of temperature, pressure and depressurization rate on release profile of salicylic acid from contact lenses prepared by supercritical carbon dioxide impregnation. *Chemical Engineering Research and Design*, 100, 89–94. <https://doi.org/10.1016/j.cherd.2015.05.008>
- Zare Banadkouki, M. R. (2023). Selection of strategies to improve energy efficiency in industry: A hybrid approach using entropy weight method and fuzzy TOPSIS. *Energy*, 279, Article 128070. <https://doi.org/10.1016/j.energy.2023.128070>
- Zhu, J., Lu, Y., & He, Q. (2024). Recent advances on bioactive compounds, health benefits, and potential applications of jujube (*Ziziphus Jujuba* Mill.): A perspective of by-products valorization. *Trends in Food Science & Technology*, 145, Article 104368. <https://doi.org/10.1016/j.tifs.2024.104368>
- Zou, F., & Budtova, T. (2021). Tailoring the morphology and properties of starch aerogels and cryogels via starch source and process parameter. *Carbohydrate Polymers*, 255, Article 117344. <https://doi.org/10.1016/j.CARBPOL.2020.117344>